

Sampling Decisions

Michael Chertkov¹, Sungsoo Ahn², and Hamidreza Behjoo¹

¹Program in Applied Mathematics and Department of Mathematics, University of Arizona, Tucson, AZ, chertkov@arizona.edu, hamidreza.behjoo@gmail.com

²Graduate School of AI at KAIST, Republic of Korea, sungsoo.ahn@kaist.ac.kr

Abstract

In this manuscript, we introduce a novel Decision Flow (DF) framework for sampling decisions from a target distribution while incorporating additional guidance from a prior sampler. DF can be viewed as an AI-driven algorithmic reincarnation of the Markov Decision Process (MDP) approach in stochastic optimal control. It extends the continuous-space, continuous-time Path Integral Diffusion sampling technique of [1] to discrete time and space, while also generalizing the Generative Flow Network (GFN) framework of [2]. In its most basic form an explicit formulation that does not require Neural Networks (NNs), DF leverages the linear solvability of the underlying MDP [3] to adjust the transition probabilities of the prior sampler. The resulting Markov process is expressed as a convolution of the reverse-time Green’s function of the prior sampling with the target distribution. We illustrate the DF framework through an example of sampling from the Ising model – compare DF to Metropolis–Hastings to quantify its efficiency, discuss potential NN-based extensions, and outline how DF can enhance guided sampling across various applications.

1 Setting the Stage

The overarching goal of Generative AI (Gen-AI) is to generate samples from a probability distribution represented through ground-truth (GT) data. A typical Gen-AI model builds an exact representation of this distribution from GT samples; for instance, diffusion models encode the score function as a sum over GT data. Recent examples include the Iterative Denoising Energy Matching (iDEM) [4] and Harmonic Path Integral Diffusion (H-PID) [1] algorithms. In some cases notably H-PID the GT-based score alone is sufficient to generate new samples without Neural Networks (NNs); in other situations (e.g., iDEM) one subsequently trains a neural surrogate.

Beyond generative modeling, both iDEM and H-PID solve a classical statistical task: drawing independent and identically distributed (i.i.d.) samples σ from a target Gibbs Boltzmann distribution

$$p(\sigma) \propto e^{-E(\sigma)}, \quad (1)$$

where E is a known energy up to an additive constant. The canonical approach is Markov Chain Monte Carlo (MCMC). Generative Flow Networks (GFNs) [2] tackle the same Gibbs-sampling goal in a discrete-time setting, auto-regressively growing a trajectory $\emptyset = s_0 \rightarrow \dots \rightarrow s_T = \sigma$ on a directed-acyclic graph while allowing each action to depend on the entire partial history.

This manuscript in a nutshell. Decision Flow (DF) retains the sequential-growth intuition of GFN yet adds a closed-form correction that makes every trajectory exactly consistent with an arbitrary target distribution. In addition, DF can exploit heuristic growth policies for guiding the trajectory while still correcting the policy to be provably exact. We envision DF to be particularly useful as a drop-in engine for improving the modern generative-AI pipelines – diffusion models and auto-regressive transformers – which hinges on fast and accurate sampling of the target distribution.

Our contributions: (i) We extend linearly-solvable MDP theory of [3] to state spaces that grow with time and derive an explicit solution – Theorem 1, which is our main result stated in Section 3; (ii) We reinterpret that solution as a universal, analytic sampler, thereby unifying integrable control (and thus

conceptually reinforcement learning), auto-regressive construction, and probabilistic inference¹. In Section 2, we describe the place of the Decision Flow within the broader landscape of GFN, diffusion-based samplers, and integrable stochastic control.

2 Decision Flow Framework and Its Connections to Generative Flow Networks, Harmonic Path-Integral Diffusion, and Reinforcement Learning

The DF framework introduced in this manuscript provides a novel and versatile approach to guided multi-stage sampling, significantly generalizing and unifying existing generative AI methodologies, including Generative Flow Networks (GFNs) [2, 7] and Harmonic Path Integral Diffusion (H-PID) [1]. In essence, DF formulates the sampling task as a sequential decision-making problem governed by a Markov Decision Process (MDP). This viewpoint highlights both the theoretical underpinnings of DF in Applied Mathematics – via Stochastic Processes, Statistical Mechanics and Stochastic Optimal Control (SOC) – and its practical connections to the three basic concepts of the GenAI – Auto-Regressive (as in Transformers), Diffusion Models and Reinforcement Learning (RL).

Links to Generative Flow Networks: GFNs focus on incrementally constructing samples on a Directed Acyclic Graph (DAG) – therefore growing a sample in a auto-regressive fashion. The flow-based design ensures that trained Markovian flows satisfy balance conditions — for example, Detailed Balance or Trajectory Balance [8, 9] — so that the target distributions match a target distribution of interest. However, GFNs do not explicitly incorporate external guidance based on prior transition probabilities. DF addresses this gap by introducing priors as domain-specific knowledge or heuristics, which are subsequently refined through optimization.

Links to Diffusion Models and Integrable SOC: DF also aligns conceptually with H-PID, a continuous-time, continuous-space approach to sampling that employs backward-time Green (response) functions to link final (target) distributions with intermediate states. In DF, these ideas are transposed into a discrete-time, discrete-state (also growing with time) framework by using prior transition probabilities and backward Green functions to achieve consistency with the target distribution. Moreover, DF leverages techniques from Integrable Stochastic Optimal Control, following the line of work on Linearly Solvable MDPs (LS-MDPs) [3, 5, 6] and Path Integral Control [10]. In particular, the pathwise corrections to the prior, reminiscent of continuous diffusion approaches, reflect the same underlying principle: adjusting forward transitions by reference to backward probability flows.

Links to MDPs and Reinforcement Learning: DF extends connections to the Maximum Entropy (MaxEnt) and Inverse Reinforcement Learning (IRL) ideas. In MaxEnt-based MDPs [11, 12], one imposes an entropy-regularized cost that encourages exploration. GFNs were eventually linked to a deterministic variant of this framework in [7], demonstrating that adjusting the target reward (prior energy) term to account for reverse probability flows yields a target Gibbs-Boltzmann distribution. DF follows a comparable principle: it incorporates prior energies that, when corrected, align the target state distribution with the desired Gibbs-Boltzmann form. This correction step also strongly resembles continuous-space denoising diffusion in AI.

From a Reinforcement Learning (RL) perspective, DF can be viewed as a specialized RL scheme that bypasses explicit definition of actions in favor of directly working with transition probabilities (akin to deterministic MDPs). The entire array of RL methods – from policy optimization to value function approximation [13] – remains applicable, offering a rich toolbox for training or fine-tuning DF in practical settings. When external or historical data is available, DF can bootstrap from these priors, effectively reducing exploration costs and improving sample efficiency. This synergy underscores how DF blends classical SOC formulations with data-driven RL principles.

From Artificial to Physical Time: Beyond algorithmic details, DF extends RL and GFN to a fully physics-informed perspective [14]. Built on stochastic processes, statistical mechanics, and optimal control,

¹Two remarks are in order: (a) To expose this linearly-solvable core we deliberately stay NN-free in the present letter; (c) The DF exact sampler is directly relevant to many decision making applications where sequential and auto-regressive creation of a sample is advantageous, see Section 6.

DF integrates information about the target distribution with the physical growth of a sample, thereby replacing the artificial time of diffusion models with an evolution grounded in problem dynamics. This transposition of DF from an algorithmic noise scale to the true clock of the underlying process is what we mean by physics-informed AI.

3 Decision Flow: Main Theorem and Analytic Solution

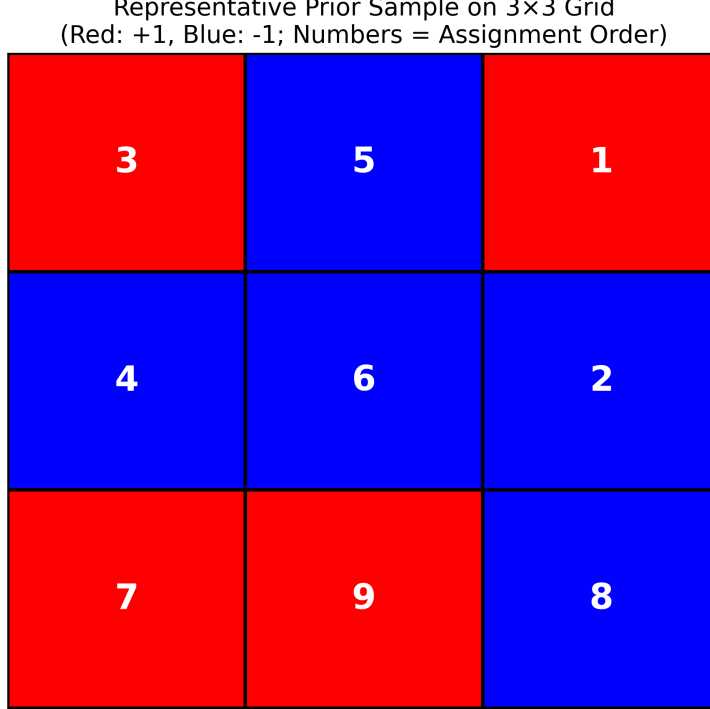


Figure 1: Representative Ising model samples generated on a 3×3 grid from the prior MP $p^{(\text{prior})}(\bullet|\bullet)$. The red and blue colors indicate spins $+1$ and -1 , respectively. The numbers within each cell show the order in which the spins were assigned during the sampling process.

We build the DF framework to address the question of i.i.d. sampling based on the queries of the energy function, $E(\sigma)$, and on the prior transition probabilities quantifying sequential growth of a sample – starting with \emptyset and at each step adding a new component to it, therefore growing a chain: $s_0 = \emptyset \rightarrow s_1 \rightarrow \dots \rightarrow s_T = \sigma$ in T steps (where the number of steps is fixed). To clarify the construction, consider an example of assigning binary values (spins) to a cell of a planar lattice, say an $n \times n$ lattice, as illustrated in Fig. 1. The initial state is $s_0 = \emptyset$. At the first step we pick one of $T = n^2$ cells, a_1 , and assign to it a spin, $\sigma_{a_1} = \pm 1$, thus generating $s_1 = \sigma_{a_1}$. The process continues so that $s_t = (\sigma_{a_1}, \dots, \sigma_{a_t})$ where $\forall t' \neq t'' \leq t, a_{t'} \neq a_{t''}$, then producing the complete sample after T steps, $s_T = \sigma = (\sigma_{a_1}, \dots, \sigma_{a_T})$. Generation of the σ -sample is therefore guided by the vector of prior transition probabilities

$$p^{(\text{prior})} \doteq (p_t^{(\text{prior})}(s_{t+1}|s_t))|t=0, \dots, T-1, \quad (2)$$

Notice that the prior MP (2) is not necessarily consistent with the target distribution (1) in the sense that the prior marginal distribution built according to Bayes' rules:

$$\pi_T^{(\text{prior})}(s_T) = \sum_{s_1, \dots, s_{T-1}} \left(\prod_{t=0}^{T-1} p_t^{(\text{prior})}(s_{t+1}|s_t) \right), \quad (3)$$

where $s_0 = \emptyset$, is not equal to $P(s_T = \sigma)$ defined according to Eq. (1). Our main result is:

Theorem 1 (Decision Flow). *Given an energy function $E(\bullet)$ and a vector of prior transition probabilities $p^{(prior)}$ such that all states with finite $E(\bullet)$ are accessible:*

(*) *A consistent vector of transition probabilities $p^*(\bullet|\bullet)$ – one that results in the marginal probability $\pi_T^*(\bullet)$ constructed according to Eq. (3) with “prior” replaced by “**” and satisfying $\pi_T^*(\sigma) \propto \exp(-E(\sigma))$ – can be obtained as follows:*

$$\begin{aligned} p_t^*(s_{t+1}|s_t) &\propto p_t^{(prior)}(s_{t+1}|s_t) \\ &\times \sum_{s'_T} \frac{e^{-E(s'_T)} G_{t+1}(s_{t+1}|s'_T)}{\pi_T^{(prior)}(s'_T)}, \end{aligned} \quad (4)$$

where $G_{\bullet}(\bullet|\bullet)$ is the Green function, initialized as

$$G_T(s_T|s'_T) = \delta(s_T, s'_T), \quad (5)$$

and recursively computed for the time-reversed process governed by the prior transition probabilities:

$$G_t(s_t|s_T) = \sum_{s_{t+1}} p_t^{(prior)}(s_{t+1}|s_t) G_{t+1}(s_{t+1}|s_T), \quad (6)$$

for $t = T-1, \dots, 0^2$.

(**) *Moreover, p^* is the optimal solution to the following Markov Decision Process (MDP):*

$$\min_{p_{0 \rightarrow T-1}, \pi_{0 \rightarrow T-1}} \mathcal{C}(p_{0 \rightarrow T-1}, \pi_{0 \rightarrow T-1}), \quad (7)$$

where the cost function is defined as: $\mathcal{C} =$

$$\sum_{t=0}^{T-1} \sum_{s_t, s_{t+1}} \pi_t(s_t) p_t(s_{t+1}|s_t) \log \left(\frac{p_t(s_{t+1}|s_t)}{p_t^{(prior)}(s_{t+1}|s_t)} \right), \quad (8)$$

subject to the dynamics and normalization constraints:

$$\pi_{t+1}(s_{t+1}) = \sum_{s_t} p_t(s_{t+1}|s_t) \pi_t(s_t), \quad (9)$$

with

$$\sum_{s_{t+1}} p_t(s_{t+1}|s_t) = 1,$$

as well as the marginal probability consistency constraint at $t = T$

$$\pi_T(s_T) \propto \exp(-E(s_T)). \quad (10)$$

Here in Eqs. (9) $t = 0, \dots, T-1$ and the initial state is given by $s_0 = \emptyset$.

The proof of Theorem 1 is presented in Section 4 and proceeds in two steps. First, we introduce a broader class of MDPs than the one defined by Eqs. (7,8,9,10), where the cost function is modified, and the consistency constraint is relaxed. In Theorem 2 – introduced in Section 4 to prove the main Theorem 1 – we show that this generalized MDP belongs to the class of Linear-Solvable Markov Decision Process (LS-MDP) type discussed in [3, 5, 6]. Second, we leverage the solution of the modified and relaxed MDP to construct a solution for the original MDP, thereby proving Theorem 1.

The practical utility of Theorem 1 is demonstrated in Section 5, where we develop an efficient algorithm for refining the prior sampler and present experimental results for sampling from an Ising model on small graphs. Finally, Section 6 summarizes our findings and discusses potential applications and future experiments using the DF framework.

²Notice that the Green function is not a proper probability distribution, $\sum_{s_t} G_t(s_t|s_T) \neq 1$.

4 Linearly Solvable MDPs

In this section, we prove Theorem 1 using Theorem 2, which generalizes results from [3, 5, 6] to accommodate a state space that grows over time. To set the stage for Theorem 2, we introduce a modified cost function:

$$\begin{aligned}\bar{\mathcal{C}}(\tau, p_{\tau \rightarrow T-1}, \pi_{\tau \rightarrow T-1}) &\doteq \sum_{s_T} \pi_T(s_T) E^{(\text{prior})}(s_T) \\ &+ \sum_{t=\tau}^{T-1} \sum_{s_t, s_{t+1}} \pi_t(s_t) p_t(s_{t+1}|s_t) \log \left(\frac{p_t(s_{t+1}|s_t)}{p_t^{(\text{prior})}(s_{t+1}|s_t)} \right).\end{aligned}\quad (11)$$

We then define a sequence of MDPs for $\tau = 0 \rightarrow T-1$:

$$\begin{aligned}\Psi_\tau(s) &= \min_{p_{\tau \rightarrow T-1}, \pi_{\tau \rightarrow T-1}} \bar{\mathcal{C}}(\tau, p_{\tau \rightarrow T-1}, \pi_{\tau \rightarrow T-1}), \\ \text{s.t. } &\text{Eqs. (9) for } t = \tau, \dots, T-1, \\ &\pi_\tau(s_\tau) = \delta(s, s_\tau).\end{aligned}\quad (12)$$

Theorem 2 (Linearly Solvable MDP). (i) The optimal values of the MDPs in Eq. (12) satisfy the following linear recurrence for $u_\tau(\bullet) \doteq \exp(-\Psi_\tau(\bullet))$:

$$\begin{aligned}u_\tau(s_\tau) &= \exp \left(-E_\tau^{(\text{prior})}(s_\tau) \right) \\ &\times \sum_{s'_{\tau+1}} p_t^{(\text{prior})}(s'_{\tau+1}|s_\tau) u_{\tau+1}(s'_{\tau+1}),\end{aligned}\quad (13)$$

initialized at $\tau = T$ with $u_T(\bullet) = \exp(-E^{(\text{prior})}(\bullet))$, and evaluated backward in time from $\tau = T$ to $\tau = 0$.

(ii) The optimal transition probabilities for $\Psi_0(\emptyset)$ are:

$$p_t^*(s_{t+1}|s_t) = \frac{p_t^{(\text{prior})}(s_{t+1}|s_t) u_{t+1}(s_{t+1})}{\sum_{s'_{t+1}} p_t^{(\text{prior})}(s'_{t+1}|s_t) u_{t+1}(s'_{t+1})}, \quad (14)$$

for $t = 0, \dots, T-1$. The corresponding marginal probabilities $\pi_\bullet^*(\bullet)$ are given by Eq. (3), replacing “(prior)” with “*”.

Proof. The proof follows the general framework outlined in [3, 5, 6], adapted to our formulation. Due to space constraints, we provide only key highlights.

Using the Hamilton-Jacobi-Bellman approach, we rewrite Eq. (12) as a sequence of recursive relations, initialized at $\tau = T$ and expressing $\Psi_{\tau-1}(\bullet)$ in terms of $\Psi_\tau(\bullet)$. These relations involve summation over s_τ and optimization over $p_\tau(\bullet, \bullet)$ and $\pi_\tau(\bullet)$, which are carried out analytically. Applying the logarithmic transformation $\Psi_\bullet(\bullet) \rightarrow u_\bullet(\bullet)$ leads to Eq. (13). Finally, extracting the corresponding arg-min expressions results in Eq. (14) and the optimal marginal probabilities. \square

Proof of Theorem 1:

Proof. We now proceed with the proof of Theorem 1. As in the proof of Theorem 2, we provide only key steps. By combining Eqs. (14,13) from Theorem 2, we obtain:

$$p_t^*(s_{t+1}|s_t) = p_t^{(\text{prior})}(s_{t+1}|s_t) \frac{u_{t+1}(s_{t+1})}{u_t(s_t)}, \quad (15)$$

for $t = 0, \dots, T-1$. On the other hand, Eq. (13) can be rewritten naturally in terms of the backward-time Green (response) functions defined in Eqs. (6,5):

$$u_t(s_t) = \sum_{s_T} G_t(s_t|s_T) e^{-E_T^{(\text{prior})}(s_T)}, \quad (16)$$

Algorithm 1 Decision Flow Sampler

Require: $\{p_t^{(\text{prior})}\}_{t=0}^{T-1}$, $E(\cdot)$, path budget K
Ensure: posterior transitions $\{p_t^*\}_{t=0}^{T-1}$

- 1: Generate K prior paths $\Xi^{(k)} = (s_0 = \emptyset, s_1^{(k)}, \dots, s_T^{(k)}), k = 1, \dots, K$ using $p^{(\text{prior})}$
- 2: Estimate empirical $\hat{p}_t^{(\text{prior})}(s_{t+1} | s_t)$ from the paths
- 3: Compute $\pi_T^{(\text{prior})}$ via Eq. (3) and the Green functions G_t backward via Eq. (6)
- 4: **for** $t = 0$ to $T - 1$ **do**
- 5: $p_t^*(s_{t+1} | s_t) \leftarrow$ Eq. (4) with $\hat{p}_t^{(\text{prior})}$
- 6: **end for**
- 7: **return** $\{p_t^*\}$

for $t = T, \dots, 0$. Substituting Eq. (15) into the expression for the optimal marginal probability yields:

$$\pi_t^*(s_t) = \frac{u_t(s_t)}{u_0(\emptyset)} \pi_t^{(\text{prior})}(s_t), \quad t = 1, \dots, T. \quad (17)$$

So far in the proof, we have only considered the MDPs in Theorem 2. Now, we establish the connection to the MDP in Theorem 1. The consistency condition (10) in Theorem 1, which ensures that the marginal probability at $t = T$ equals the target probability, corresponds directly to the prior energy term $E(\bullet)$ in the cost function of Theorem 2 defined in Eq. (11)³. Evaluating Eq. (17) at $t = T$ and combining it with Eq. (16) leads to:

$$e^{-E(s_T)} \propto \frac{\pi_T^{(\text{prior})}(s_T) e^{-E_T^{(\text{prior})}(s_T)}}{\sum_{s'_T} G_0(\emptyset | s'_T) e^{-E_T^{(\text{prior})}(s'_T)}}.$$

Inverting this relation gives an explicit expression for $E_T^{(\text{prior})}(\bullet)$ in terms of $E(\bullet)$ and $\pi_T^{(\text{prior})}(\bullet)$:

$$E_T^{(\text{prior})}(s_T) = E(s_T) + \log \pi_T^{(\text{prior})}(s_T) + \text{const.} \quad (18)$$

Combining these results, we arrive at the main statement of the theorem, Eq. (4). The remaining statements of the theorem follow naturally from the explicit transformations derived above. \square

Note that unlike [3, 5, 6], Theorem 1 (i) admits a time-growing state graph, (ii) yields the convolution form (4), and (iii) proves optimality with respect to KL-divergence to the target sampler.

5 Explicit NN-Free Decision Flow Algorithm

The theoretical result in Theorem 1 provides a principled mechanism to correct any prior sampling process toward exact sampling from a target distribution. In practice, the decision-flow theory is distilled into the explicit **Algorithm 1** which implements this correction empirically: we generate a batch of samples from the prior, estimate the required Green function and terminal marginal (Eq. 3 and Eq. 6), and substitute these into the convolution formula (Eq. 4). This means the empirical prior replaces the theoretical prior in Theorem 1, and thus the algorithm approximates the analytic solution. While the original theorem assumes known priors and exact marginals, the approximation becomes accurate with increasing path budget K , as exemplified later in the Section on the example of sampling from the Ising model (see Fig. 2). This practical translation is consistent with how Theorem 1 was derived. Note also that the Algorithm is intentionally NN-free⁴.

Graphical Model Sampling: In addition to its primary application in drug discovery, the GFN approach has also been tested on a combinatorial optimization problem, where high-probability states emerge through

³It is crucial – to prevent singularities and ensure that the formulations the theorems are equivalent – that the prior assigns a strictly positive probability to every state in the target distribution Eq. (1).

⁴Replacing the analytically computed Green factors with neural surrogates leaves the algorithmic structure unchanged yet enables high-dimensional applications such as image or molecule generation. See Section 6.

a sequential growth process from an empty set to the desired sample [15]. Specifically, [15] examined the efficiency of growing an independent set over a graph. This example, while more academic than practical, provides a sufficiently rich setting to evaluate GFN performance. Notably, the focus of [15] was not on sampling but rather on solving a combinatorial optimization problem – finding the Maximum Likelihood (ML) independent set. This is somewhat at odds with the original motivation behind GFN – designed to sample i.i.d. from the target distribution rather than to find the most probable sample⁵.

Since we design DF for sampling and wish to adhere to this objective, we deviate from the approach in [15] and focus on the original problem – sampling i.i.d. from the target distribution. Moreover, we concentrate on sampling from the Ising model rather than an independent set problem considered in [15].

We illustrate the Explicit DF sampling algorithm on the Ising model over an undirected graph $\mathcal{G} = (\mathcal{V}, \mathcal{E})$, where \mathcal{V} and \mathcal{E} are the sets of nodes (vertices) and edges, respectively. Our goal is to generate samples, $\sigma = (\sigma_a = \pm 1 | a \in \mathcal{V})$, i.i.d. from the distribution defined in Eq. (1) with the Ising energy

$$E(\sigma) = - \sum_{(a,b) \in \mathcal{E}} J_{ab} \sigma_a \sigma_b - \sum_{a \in \mathcal{V}} h_a \sigma_a, \quad (19)$$

where the pairwise interaction terms $J = (J_{ab} | (a,b) \in \mathcal{E})$ and singleton biases $h = (h_a | a \in \mathcal{V})$ are assumed to be given. The algorithm is implemented in two steps:

(1) **Building MP Prior** – $p^{(\text{prior})} = (p_t^{(\text{prior})}(s_{t+1} | s_t) | t = 0, \dots, T-1)$: We construct $p^{(\text{prior})}$ as a Markov Process that generates a sample path Ξ according to the following rule: Define a sequence of partial assignments $s_0 = \emptyset$, s_1, s_2, \dots, s_N , where s_t represents the configuration after t steps and $N = |\mathcal{V}|$. Initialize with $V_0 = \emptyset$, $E_0 = \emptyset$. At each step $t = 0, \dots, N-1$, choose a new node $a_{t+1} \in \mathcal{V} \setminus V_t$ and assign it a spin $\sigma_{a_{t+1}} \in \{+1, -1\}$ according to

$$\sigma_{a_{t+1}} \sim \text{softmax} \left(\left\{ \tilde{h}_b \sigma_b : b \in \mathcal{V} \setminus V_t, \sigma_b \in \{+1, -1\} \right\} \right),$$

where the effective bias is given by

$$\tilde{h}_b = h_b + \sum_{\substack{a \in \mathcal{V}_t \\ (a,b) \in \mathcal{E}}} J_{ab} \sigma_a.$$

After sampling, update the visited set $V_{t+1} = V_t \cup \{a_{t+1}\}$ and define the new state by

$$s_{t+1} = (s_t, \sigma_{a_{t+1}}).$$

The complete sample is then $\sigma = s_N = (\sigma_{a_1}, \sigma_{a_2}, \dots, \sigma_{a_N})$, which is generated by the prior

$$p_{\text{prior}} = \left\{ p_{\text{prior}}(s_{t+1} | s_t) \right\}_{t=0}^{N-1} \quad (6)$$

(2) **From MP Prior to MDP Posterior**: Once the MP prior is built we use it to generate K prior samples and then utilize the general scheme above to devise the empirical expressions for the posterior transition probabilities. Then we generate S posterior samples to validate the method and verify its performance against an exact or MCMC benchmark.

Experiments with the DF Algorithm:⁷ We test the DF algorithm on a small “glassy” Ising model. Fig. 1 illustrates a representative prior sample. Using K prior samples, the DF algorithm generates S posterior (target) samples. To assess sample quality, we compute empirical estimates of the singleton and pairwise correlations:

$$m_a^* = \frac{1}{S} \sum_{s=1}^S \sigma_{T;a}^{(s)}, \quad c_{ab}^* = \frac{1}{S} \sum_{s=1}^S \sigma_{T;a}^{(s)} \sigma_{T;b}^{(s)},$$

⁵Our hypothesis is that the authors of [15] chose to apply GFN to the ML problem to align with more standard benchmarks. ML estimation in discrete settings has historically received more attention than the more challenging sampling problem.

⁶Note that although this sequential scheme is inspired by the target Gibbs-Boltzmann distribution Eq. (1) for the Ising model defined in Eq. (19), the prior process itself does not yield i.i.d. samples from $p(\sigma)$.

⁷Code is available at <https://github.com/hamidrezabehjoo/DecisionFlow>.

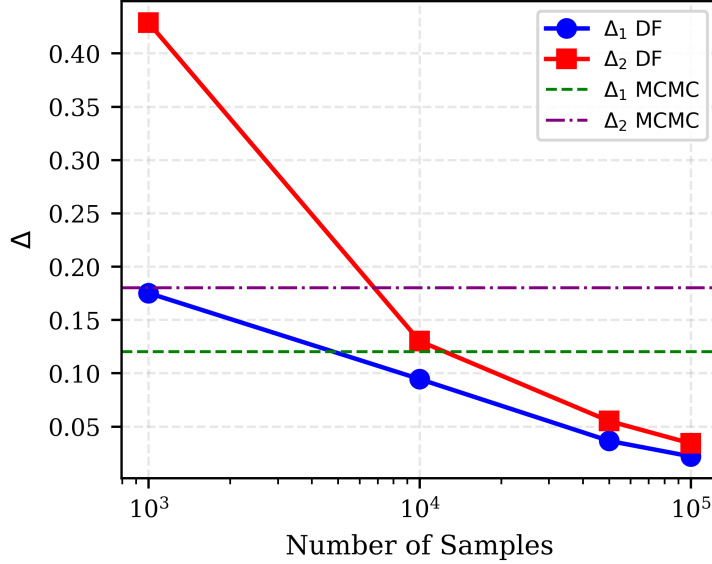


Figure 2: Accuracy-effort trade-off of DF versus a tuned Metropolis–Hastings (MH) baseline on a 3×3 ‘glassy’ Ising grid with $h_a, J_{ab} \sim \mathcal{U}[-1, 1]$. The solid lines show the convergence of the DF-corrected sampler (approximating Theorem 1) as the number of paths increases. Dashed lines mark the accuracy reached by MH after 2,000 burn-in sweeps followed by 5,000 recorded samples (one kept every ten sweeps). DF attains the same error level at $K = S \approx 5 \times 10^4$ paths – more than two orders of magnitude fewer evaluations than consumed by MH.

and compare them to reference values – obtained either exactly (as in the 3×3 example) or via MCMC. The integrated mismatch metrics are defined as

$$\Delta_1 = \sum_a \frac{\|m_a - m_a^{(\text{ref})}\|}{T \|m_a^{(\text{ref})}\|}, \quad \Delta_2 = \sum_{(a,b)} \frac{2\|c_{ab} - c_{ab}^{(\text{ref})}\|}{T(T-1) \|c_{ab}^{(\text{ref})}\|}.$$

Our results demonstrate that, with a sufficiently small sample size, the DF algorithm outperforms MCMC⁸. See Fig. 2 for the Δ -test results and Fig. 3 for the energy probability density function of the generated samples.

6 Conclusions and Path Forward

In this work we introduced the DF framework, bridging MDP, GFN, and physics-informed sampling. By correcting a prior sampler with a convolution of the Green function with the target distribution, DF achieves i.i.d. sampling from complex targets without relying on NNs.

Why DF qualifies as physics-informed AI? Because the prior kernel can encode real-time dynamics – e.g., Euler time-steps in fluid mixing or hourly unit-commitment schedules – DF enforces consistency with those dynamics rather than an artificial diffusion clock. The Green-function governed correction leaves that physical timeline intact.

Looking ahead we envision NN Extensions: In high-dimensional settings the Green functions, and more generally posterior transition probabilities, can be amortized by a neural surrogate, trained with a noise-free target provided by Theorem 1. This yields an NN-powered DF that retains the theoretical guarantees of the analytic solution while scaling to large problems. A first implementation is underway.

DF’s ability to embed domain priors suggests promising applications in infrastructure scheduling, epidemiological simulation, and physics-constrained process control which we briefly discuss next.

⁸Note that DF exemplifies the broader class of time-inhomogeneous diffusion samplers; empirical studies consistently show these methods to be more flexible and substantially more sample-efficient than classical MCMC, although a complete theoretical explanation is still an open problem.

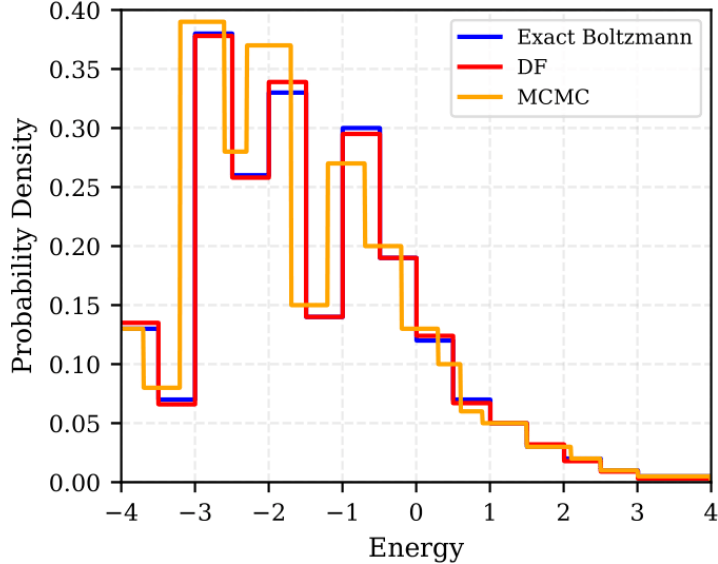


Figure 3: Probability density function of the energy $E(\sigma)$ estimated from DF-generated samples. The density is computed from σ samples produced using the DF algorithm with $K = S = 5 \times 10^4$, under the same experimental conditions as described in Fig. 2.

Towards New Applications: By establishing DF as a flexible and modular framework, we open avenues for its application across a diverse set of real-world problems where probabilistic sampling plays a crucial role. Below, we highlight key areas where DF can be particularly impactful:

6.0.1 Unit Commitment in Infrastructure Systems

The DF framework can enhance optimization and control strategies for large-scale systems such as energy and transportation networks. By dynamically adjusting prior transition probabilities, DF can provide robust and scalable solutions for scheduling and resource allocation.

6.0.2 Preventing Outbreaks and Sampling Paths

In epidemiological modeling, DF enables efficient identification of high-risk pathways for disease spread. By leveraging historical infection patterns and real-time data, DF can assist in mitigating potential outbreaks, whether in viral pandemics or social contagions. The DF methodology extends naturally to agent-based modeling of epidemiological spread. Given a city represented as a geo-graph, DF can adaptively learn and refine transition probabilities, capturing both historical mobility patterns and real-time assessments of infection risk.

6.0.3 Process Control

Applications in materials science and fluid dynamics stand to benefit from DF’s ability to guide complex processes with embedded physical constraints. Examples include optimizing reaction pathways in chemical engineering or controlling mixing or temperature in fluids.

In conclusion – uniting theoretical rigor with applications, the DF framework presents a compelling approach to physics-informed AI, offering opportunities for structured sampling in domains where uncertainty, dynamics, and decision-making intersect.

References

- [1] H. Behjoo and M. Chertkov, “Harmonic path integral diffusion,” *IEEE Access*, vol. 13, pp. 42196–42213, 2025.
- [2] E. Bengio, M. Jain, M. Korablyov, D. Precup, and Y. Bengio, “Flow Network based Generative Models for Non-Iterative Diverse Candidate Generation,” Nov. 2021. arXiv:2106.04399.
- [3] E. Todorov, “Linearly-solvable Markov decision problems,” in *Advances in Neural Information Processing Systems*, vol. 19, pp. 1369–1376, MIT Press, 2007.
- [4] T. Akhoud-Sadegh, J. Rector-Brooks, A. J. Bose, S. Mittal, P. Lemos, C.-H. Liu, M. Sendera, S. Ravanbakhsh, G. Gidel, Y. Bengio, N. Malkin, and A. Tong, “Iterated Denoising Energy Matching for Sampling from Boltzmann Densities,” June 2024. arXiv:2402.06121.
- [5] K. Dvijotham and E. Todorov, “A Unifying Framework for Linearly Solvable Control,” Feb. 2012. arXiv:1202.3715.
- [6] M. Chertkov, V. Y. Chernyak, and D. Deka, “Ensemble Control of Cycling Energy Loads: Markov Decision Approach,” Oct. 2017. arXiv:1701.04941.
- [7] T. Deleu, P. Nouri, N. Malkin, D. Precup, and Y. Bengio, “Discrete Probabilistic Inference as Control in Multi-path Environments,” May 2024. arXiv:2402.10309.
- [8] K. Madan, J. Rector-Brooks, M. Korablyov, E. Bengio, M. Jain, A. Nica, T. Bosc, Y. Bengio, and N. Malkin, “Learning GFlowNets from partial episodes for improved convergence and stability,” June 2023. arXiv:2209.12782.
- [9] H. Jang, M. Kim, and S. Ahn, “Learning Energy Decompositions for Partial Inference of GFlowNets,” Oct. 2023. arXiv:2310.03301.
- [10] H. J. Kappen, “Path integrals and symmetry breaking for optimal control theory,” *Journal of Statistical Mechanics: Theory and Experiment*, p. P11011, 2005.
- [11] B. D. Ziebart, A. L. Maas, J. A. Bagnell, and A. K. Dey, “Maximum Entropy Inverse Reinforcement Learning,” in *Proceedings of the 23rd AAAI Conference on Artificial Intelligence (AAAI-08)*, pp. 1433–1438, AAAI Press, 2008.
- [12] S. Levine, “Reinforcement Learning and Control as Probabilistic Inference: Tutorial and Review,” May 2018. arXiv:1805.00909.
- [13] R. S. Sutton and A. G. Barto, *Reinforcement Learning: An Introduction*. The MIT Press, 2nd ed., 2018.
- [14] M. Chertkov, “Mixing artificial and natural intelligence: from statistical mechanics to AI and back to turbulence,” *Journal of Physics A: Mathematical and Theoretical*, vol. 57, p. 333001, Sept. 2024.
- [15] D. Zhang, H. Dai, N. Malkin, A. Courville, Y. Bengio, and L. Pan, “Let the Flows Tell: Solving Graph Combinatorial Optimization Problems with GFlowNets,” Nov. 2023. arXiv:2305.17010.